UNIVERSITY OF LEEDS

Article:
Luhaib, S orcid.org/0000-0002-6170-5114, Somjit, N orcid.org/0000-0003-1981-2618 and Hunter, I orcid.org/0000-0002-4246-6971 (2018) Spurious Stopband Improvement of Dual-Mode Dielectric Resonator Filters Using T-shaped Coupling Probe. IET Microwaves, Antennas and Propagation. ISSN 1751-8725

https://doi.org/10.1049/iet-map.2018.5296

IET Microwaves, Antennas & Propagation

Spurious Stopband Improvement of Dual-Mode Dielectric Resonator Filters Using T-shaped Coupling Probe

MAP-2018-5296 | Research Article

Submitted on: 14-05-2018

Submitted by: Saad Wasmi Osman Luhaib, Nutapong Somjit, Ian Charles Hunter

Keywords: MICROWAVE FILTERS, DUAL-MODE RESONATORS AND FILTERS, SPURIOUS MODE SUPPRESSION, DIELECTRIC RESONATOR

IET Research Journals

Submission Template for IET Research Journal Papers

IET Journals
The Institution of Engineering and Technology

ISSN 1751-8644
doi: 0000000000
www.ietdl.org

Spurious Stopband Improvement of Dual-Mode Dielectric Resonator Filters Using T-shaped Coupling Probe

Saad W. O. Luhaib[1,2], Nutapong Somjit[1], Ian C. Hunter[1]

[1] *School of Electronic and Electrical Engineering, University of Leeds, UK*
[2] *Electrical Engineering Department, University of Mosul, Mosul, Iraq*
* *E-mail: elswol@leeds.ac.uk, saadw1981@gmail.com*

Abstract: This paper presents a new design technique for dual-mode dielectric loaded resonator filter operating at 2.18GHz by using T-shape coupling probe. A cylindrical dielectric puck is suspended in the middle of metallic cavity and short-circuited on the side walls. Four vertically etched-slots through the dielectric puck from the top to the base of the ceramic puck offer a high unloaded quality factor of 4300 at the fundamental $TE_{11\delta}$ mode and allows the T-shape coupling to be located close to the centre of the dielectric puck. The size reduction ratio in this resonator was 11% compared with air filled coaxial resonator. Fourth-poles Chebyshev bandpass filter (BPF) with planar configuration was designed and implemented by employing two dielectric-loaded cavities. The experimental results show that the spurious-free window of approximately 820 MHz from the fundamental frequency of 2.18GHz and the operational bandwidth of 77 MHz were achieved.

1 Introduction

Dielectric resonator (DR) filters are widely utilised in modern microwave communication systems because of high Q-factor and good thermal stability [1, 2]. Due to the increasing figure-of-merit demand for wireless communication systems and crowded frequency spectrum, filter optimization becomes crucial. This entails requirements for high Q values, small size, minimal insertion loss and large spurious-free window. Single-mode DR resonator filter can achieve superior figure-of-merit, e.g. low signal losses [4, 5] as well as decrease overall size of the filter structures [3]. Moreover, dual-degenerate mode in dielectric-loaded cavity filter was reported with size reduction ratio of 8.3% compared with standard TE_{111} [6]. Recently, the resonator design technique consisting of a half-cut cylindrical ceramic puck, to reduce the overall filter size, exhibiting dual-mode performance at certain diameter/height (D/L) ratio was reported [7]. However, the spurious-free window from that design achieves only 600 MHz by using a four-pole bandpass filer and a 50% size reduction was obtained compared with HEH_{11} dual mode. Moreover, no significant improvement has been achieved in any previously published works based on the size reduction and the spurious behaviour. In [8] a new class of dual mode DR filter with high Q factor and good spurious-free window was presented. However, the measured results show a high insertion loss about 2.1 dB due to the coupling mechanism used and imperfection in contact between the ceramic puck and the metallic housing. Also, the spurious-free window was decreased from 770 MHz in eigen-mode analysis to 350 MHz for fourth-order filters.

This paper presents a new design technique for dual-mode loaded-cavity resonator operating at 2.18GHz by using T-shape coupling probe to achieve a small size filter with a high spurious-free window without compromising any figure of merits. The DR structure featuring a dielectric puck located in the middle of a metallic cavity with air space below and above the puck of ceramic and short-circuited along the side wall of the cavity. The $TE_{11\delta}$ is the fundamental resonance mode for the dual-degenerate mode. Vertically etched holes, in combination with slots were implemented from the top to the base of the dielectric puck for the effective input/output coupling because the E-field is concentrated in the middle of the DR structure. The resonator in this work is ultra-compact with size reduction ratio of 11% compared to air filled coaxial filter. The spurious-free window was doubled compared with $TE_{11\delta}$ dual mode in [8]. A four-pole Chebyshev filter was designed and measured with a new EM coupling mechanism, which confirms the validity of the new design approach introduced in this work.

2 Dual-mode Resonator Configuration

Fig. 1 shows the configuration of the dual mode DR with a cross section of the dielectric structure. The resonator consists of a thick ceramic puck with a high dielectric constant suspended in the middle of a cylindrical metallic cavity and short circuited along the side wall. D and L are the diameter and length of the DR respectively, while L_a is the vertical size of the air gap above and below the puck. The vertically etched slots and holes through the dielectric puck are implemented with dimensions r_0, d_x and L_x to improve the Q factor and make a good space for effective I/O coupling. The ceramic material used in this work is barium titanate with a relative permittivity of 43 and loss tangent of 4×10^{-5}. The metal cylindrical cavity is made from copper with conductivity 4×10^7 S/m. In order to choose the optimum dimensions for the proposed resonator, HFSS software was used to calculate the resonance frequency and

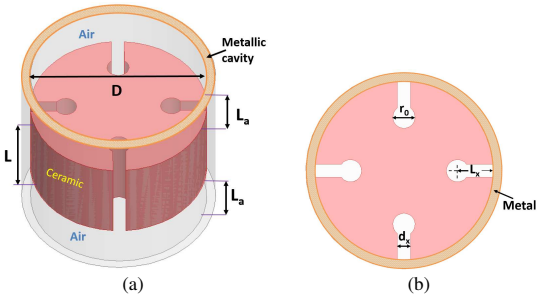

Fig. 1: Configuration of dual mode dielectric resonator
a 3D-view
b Top view

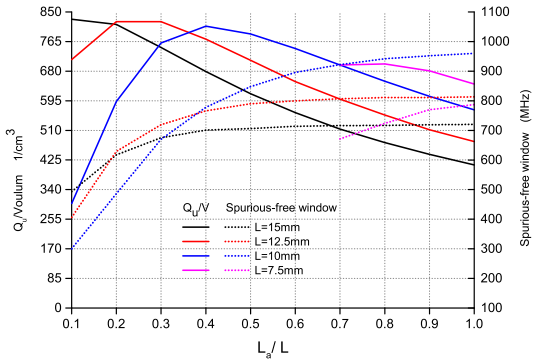

Fig. 2: The ratio of Q_u/V and spurious-free window against of the ratio of L_a/L.

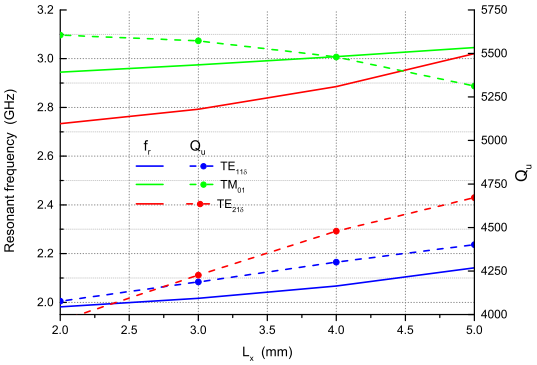

Fig. 3: Resonance frequencies and Q_u with varying slot length L_x.

unloaded Q factors (Q_u) for DR. By varying the dimensions of DR at certain frequency and analysing the features of DR (volume, Q_u and spurious-free window). Fig. 2 illustrates the relation between ratio of the the height of air space/height of ceramic (L_a/L) against the factor of Q_u/Volume(V) for the left axis and spurious-free window for right axis at the dual mode resonance frequency 2 GHz. Q_u/V is a reliable term for indicating a high Q_u and small volume of the resonator. It is worthy to note that at height when resonator (L) equals to 7.5 mm, there is no data on the graph under L_a/L less than 0.7, these happened because the resonance frequency at these value are more than 2 GHz. The highest value of spurious-free window for all conditions of L is 10 mm , which is about 100 MHz higher than other dimensions. The optimum dimensions at range 0.4-0.6 which gives a good trade off among the Q_u, volume and spurious-free window. The optimum dimensions are D=20 mm,L=10 mm and L_a=5mm. In order to have a proper space with applicable practical dimensions for the T-shape probe, the notching dimensions r_0 and d_x have been chosen to be 2.5 mm and 1.48 respectively. The optimum value of length of slot (L_x) can be found by measuring the resonant frequency and Q_u with variation of L_x. Fig. 3 illustrates the variation of the resonant frequency and Q_u of the first three modes against L_x. From the plot, the resonant frequencies for TE modes have gradually increased with L_x while the Q_u of the TM mode decreased. Choosing L_x equal to 4 mm provides a good trade off between the spurious frequency and Q_u because the spurious-free window slightly changed after this dimension. Table 1 illustrates the figure-of-merit comparison between unpatterned (UNP) and vertically-etched (V-E) DRs based on the simulated resonant frequency(f_r), unloaded Q-factor (Q_u) and the type of mode for the first three modes.

Table 1 Comparison of simulated resonance frequency, mode type and Q_u for the cavity resonator with unpatterned and vertically-etched structures

Mode	f_r(GHz)		Q_u-factor		Type	
	V-E	UNP	V-E	UNP	V-E	UNP
$TE_{11\delta}$	2.066	1.92	4300	3800	Dual	Dual
$TE_{21\delta}$	2.885	2.69	4480	3500	Dual	Single
TM_{01}	3	2.85	5480	5000	Single	Single

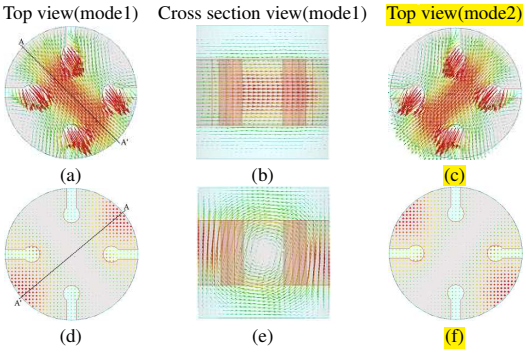

Fig. 4: Field patterns of the fundamental mode 2.06 GHz.
a-c Electric field
e-f Magmatic field

From the table, the $TE_{21\delta}$ is in single mode while it was dual mode in the UNP dielectric-puck design caused by the 4 V-E and holes in the design structure which improve the spurious-free window when two or more cavity filters are used. The overall spurious-free window is 880 MHz from the fundamental frequency achieving a larger spurious-free window and Q-factor compared to the UNP DR. The electric and magnetic field patterns of the $TE_{11\delta}$ mode at 2.066 GHz are shown in Fig. 4. It is clear that high E-field concentration around the vertically etched holes and slots can be used for efficient I/O coupling and the section $A - A^{'}$ in Fig. 4a shows the direction of E-field for mode 1 to etching hole while maintaining constant concentration in the middle. The behaviour of E-field for mode 2 in Fig. 4c, it is similar to the E-field pattern in mode 1 with 90^0 phase shift. However, the behaviour of the H-field pattern is similar in both the top view and the $A - A^{'}$ section as illustrated in Fig. 4b, when it is compare to the UNP DR design. To design filter we need to know the coupling value for external, inter-resonator and the inter- cavity. The next section will discuss the methods and the shape required to achieve the filter specification to be implemented.

2.1 External Q factor

A T-shaped probe is employed to provide the efficient EM-signal coupling for the input and output ports, as depicted in Fig. 5. The probe length L_m was used to control the EM coupling by varying the diameter of the probe. A diameter of 2 mm has been chosen to obtain a proper gap between the side of the DR and the probe to avoid over coupling when there is a direct contact between them. The group delay method is used to calculate Q_e, is given by [9].

$$Q_e = \frac{\pi f_0 \tau_D}{2} \quad (1)$$

where the τ_D is the group delay at the resonant frequency f_0. Fig. 6 illustrates the Q_e for various lengths of L_m. From the graph, an inversely proportional relationship is discovered between the external coupling and the probe length.

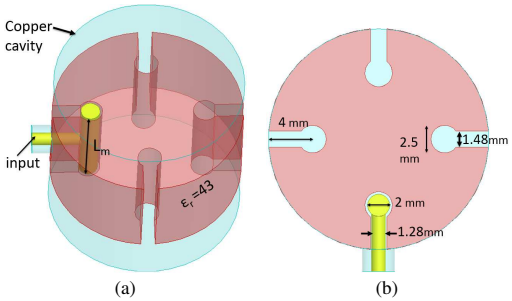

Fig. 5: Configuration of I/O coupling for dual-mode resonator
a 3D-view
b Top view

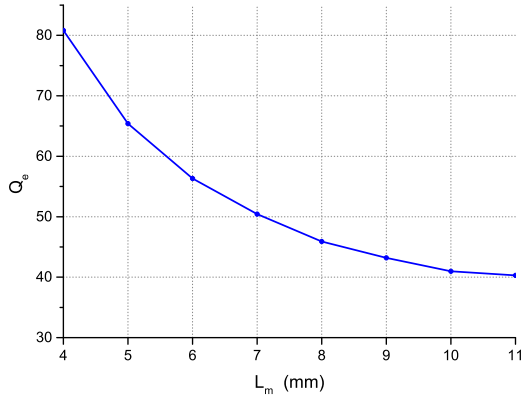

Fig. 6: The external quality factor (Q_e) against L_m.

2.2 *Inter-Resonator Coupling*

A vertically etched hole at 45^0 w.r.t degenerate modes is employed to achieve efficient EM inter-resonator mechanism coupling. Eigenmode simulation has been used to determine and synthesize the inter-resonator coupling in the DR cavity.

Fig. 7 shows the coupling bandwidth against distance between the centre of the DR and the coupling hole (X_f) with variations in the vertically-etched hole radius (re). From the plot, there are two distinct and contradictory regions of behaviour in the graph converging at X_f=5 mm . The coupling bandwidths increase significantly as X_f increases in region one ($X_f < 5$ mm) but gradually decrease in area two. Furthermore, a maximum coupling bandwidth of 110 MHz occurs at X_f is 5 mm which is caused by a maximum E-field close to the I/O coupling etched holes.

2.3 *Inter-Cavity Coupling*

Fig. 8 presents the configuration of inter-cavity coupling. This was achieved by changing the length of probe L_n to obtain the specific value of the coupling. In order to connect the two cavities, the probe was placed in a rectangular air-filled cavity with dimensions of 4 mm×4 mm×6 mm. Fig. 9 shows the inter-cavity coupling bandwidth against L_n. From the plot, L_n has a strong effect on the coupling bandwidth and it is a linearly proportional relationship. A positive slope of 10 MHz/mm is observed.

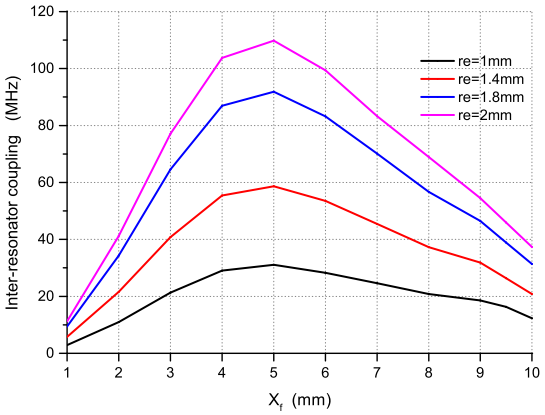

Fig. 7: Inter-resonator coupling bandwidth against X_f.

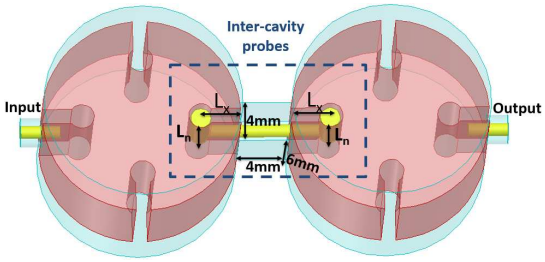

Fig. 8: Configuration of intra-cavity coupling in dual-mode

3 Filter Design with T-shaped Probe

Following the above coupling calculations, the filter is designed and fabricated. Fig. 10 displays the physical configuration of the dual-mode 4^{th} order filter with T-shaped coupling. The metallic cavity and all the probes were fabricated from copper with conductivity about 4×10^7 S/m. The two-ceramic pieces with ϵ_r=43 and $\tan\delta = 4 \times 10^{-5}$ were placed in the middle of the copper cavity and short-circuited along the side wall. The coaxial probe L_m was used for I/O coupling and L_n control the inter-cavity coupling. The vertically-etched hole through the DR was used to introduce the inter-resonator coupling. A fourth-order Chebyshev dual-mode filter was designed at centre frequency of 2.08 GHz, with operational bandwidth of 66 MHz and return loss (L_R) of better than 20 dB. The normalized coupling matrix (M) was generated without any non-adjusted coupling between the resonators as shown below.

$$M = \begin{bmatrix} & S & 1 & 2 & 3 & 4 & L \\ S & 0 & 1.035 & 0 & 0 & 0 & 0 \\ 1 & 1.035 & 0 & 0.91 & 0 & 0 & 0 \\ 2 & 0 & 0.91 & 0 & 0.7 & 0 & 0 \\ 3 & 0 & 0 & 0.7 & 0 & 0.91 & 0 \\ 4 & 0 & 0 & 0 & 0.91 & 0 & 1.035 \\ L & 0 & 0 & 0 & 0 & 1.035 & 0 \end{bmatrix}$$

The input and output external quality factors and coupling coefficients were computed for fractional bandwidth (FBW)=2.173% , and found to be M_{12}=M_{34}= 60.1 MHz, and Q_e=30. From Fig. 6, the length of the L_m probe required to obtain the exact external quality factor is 10 mm, where the internal coupling is depicted in Fig. 7. The diameter of the vertically etched hole is 4.4 mm and it is located at 9.5 mm from the centre of the dielectric puck, and the M_{23}=46.2

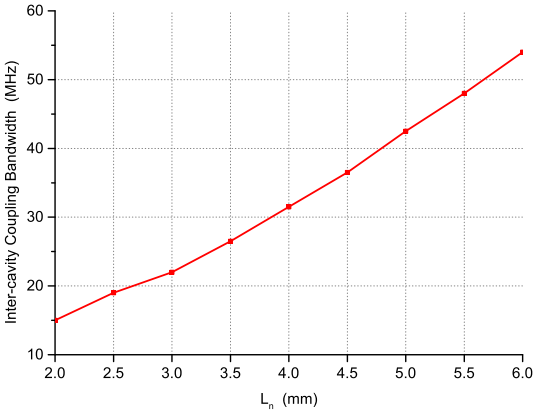

Fig. 9: Inter-cavity coupling bandwidth against L_n.

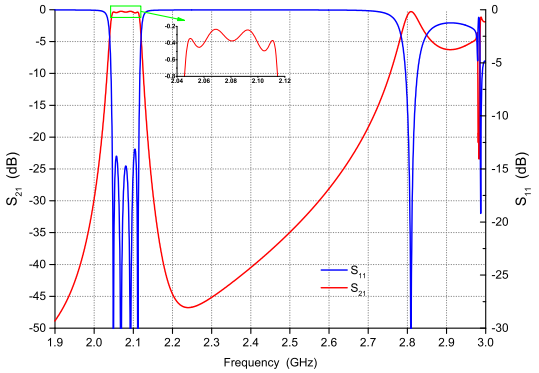

Fig. 11: Simulated spurious response of 4^{th}-order T-shape coupling filter.

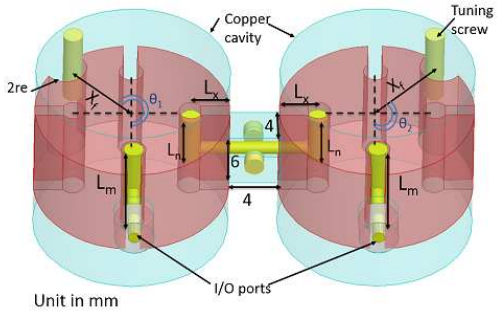

Fig. 10: T-shape coupling configuration of 4^{th}-order dual-mode filter.

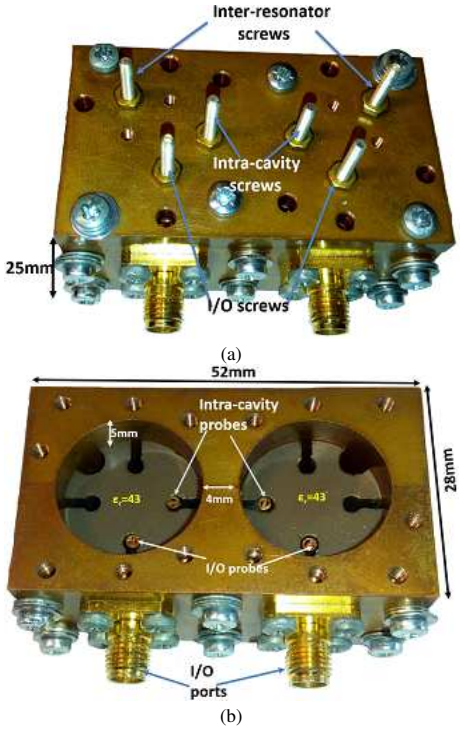

Fig. 12: Fabricated of 4^{th} degree dual-mode bandpass filter
a close with top lid
b open without top lid

MHz, L_n is 5.2 mm. The orientations of the inter-resonator coupling holes were $\theta_1 = 225^0$ and $\theta_2 = 135^0$, as shown in Fig. 10.

Fig. 11 shows the spurious response of the 4^{th} order T-shape coupling filter. From the plot, the bandwidth of the filter measured at L_R=14 dB was equal to 66.5 MHz. The insertion (IL) loss at the operational frequency 2.08 GHz is less than 0.375 dB and the extracted unloaded Q factor is more than 3700 with losses in the Q_u of approximately 500. The maximum out of band rejection in the upper side is approximately 47 dB, which is found at 2.239 GHz. The first spurious mode is at approximately 2.8 GHz and in a good agreement with the eigen-mode analysis. Furthermore, the third spurious mode is at 3 GHz. The overall spurious-free window is at approximately 720 MHz which is a superior suppression compared with the conventional dual-mode DR filter.

4 Experimental Results

Fig. 12 provides a photograph illustrating the fabrication of the 4^{th}-order dual -mode DR T-shaped coupling filter. The dimensions of the rectangular filter are 56 mm×28 mm× 25 mm, while the other cavity dimensions and the properties of the material are exactly the same as mentioned in section 3. Six tuning screws of 2 mm in diameter were positioned on the top lid of the cavity to fine-tune the coupling coefficients and all probes were fabricated out of copper. The etching holes have been done by a cutting laser machine. The probes ware covered by plastic foil to avoid the over coupling when the probe touches the DR. S-parameter measurement is achieved by using an Agilent E5071C Network Analyzer. Two-port calibration is performed by using the Agilent N4431-60006 Electronic Calibration Module prior to the measurement.

Fig. 13 shows the measured results of the filter at the wideband response. From the measurements, the insertion loss is approximately 0.42 dB at the operational frequency of 2.18 GHz with the operational bandwidth of 77 MHz at the L_R=15 dB. The extracted

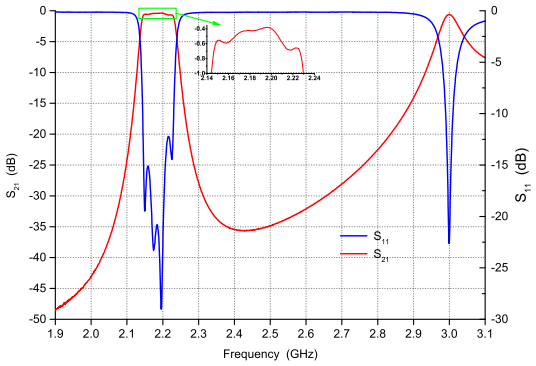

Fig. 13: Measured response of the T shape coupling filter

Q_u from the response, based on the measurement results, is approximately 2200. There were frequency shifts of 100 MHz and 11 MHz in the operational frequency and bandwidth, respectively, compared with the simulation results. Due to the tolerance of the fabrication, the frequency shifting is caused by the gap between the ceramic puck and the wall of the copper cavity as shown in Fig. 14. It can be seen that the gap around the ceramic puck has a significant effect on the resonant frequency. In this case: about 90 μm gap could push the frequency to be 2.18 GHz. The bandwidth shifting is caused by the tolerance of the fabrication in X_f and re for vertically etched hole. There are many reasons for the loss in the fabricated filter prototype. Firstly, the non-uniform gap between the ceramic and the cavity wall. Secondly, the plastics foil that have been used to insulate the probes to avoid contact with the DR as displayed in Fig. 15. Moreover, the extracted Q_u from simulation result about 2500 which is closed to the practical result. The spurious signal occurs at 3 GHz. The $TE_{21\delta}$ shifted up to about 150 MHz and the overall spurious-free window remained at 820 MHz.

Fig. 16 shows the S-parameter for the T-shaped 4th-order when the ceramic is covered and not covered by aluminium foil. From the plot, the resonance frequency shifted down to about 50 MHZ compared with the uncovered ceramic while the Bw remained the same. The IL at the resonance frequency was about -2.8 dB, which means, the losses are larger than in the first case. The losses increased because of the non-smooth layer between the ceramic and the cavity wall, which may create an air gap.

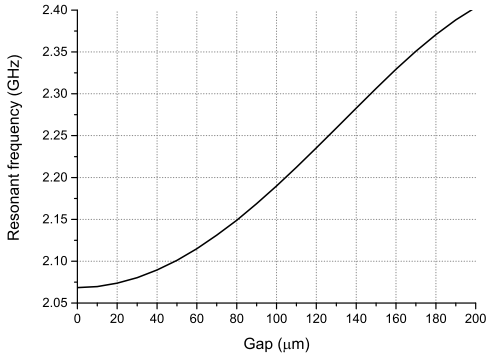

Fig. 14: Variation of gap between the metallic cavity and the DR puck against the resonant frequency.

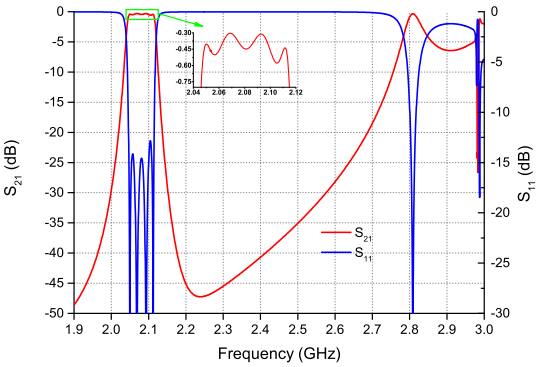

Fig. 15: Simulated spurious response of 4^{th}-order T-shape coupling filter with covered the coupling probes by plastic foil.

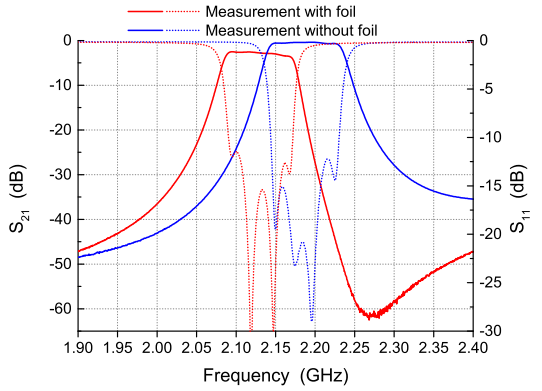

Fig. 16: Comparison of wideband response of measured T-shape coupling filter.

5 Conclusion

T-shape coupling probe for dual-mode dielectric loaded resonator filters was presented. A significant spurious-free window has been achieved compared with the same aspect. Vertically-etched slots and holes on the DR improve the Q_u and make the coupling easier without affecting the high order modes. A four-pole Chebyshev bandpass filter was designed and measured. The experimental result shows a shift upward in the resonant frequency. The coupling technique reduced the coupling to the second mode and that caused to improve the spurious-free window which was about 820 MHz.

6 References

1 Wang, C. and Zaki, K.A.: 'Dielectric Resonators and Filters', IEEE Microwave Magazine, 2007, 8, (5), pp. 115-127.
2 Hunter, I. and Engineers, I.o.E.: 'Theory and Design of Microwave Filters', (Institution of Engineering and Technology, 2001).
3 Mansour, R.R.: 'Filter Technologies for Wireless Base Stations', IEEE Microwave Magazine, 2004, 5, (1), pp. 68-74.
4 Cohn, S.B.: 'Microwave Bandpass Filters Containing High-Q Dielectric Resonators', IEEE Transactions on Microwave Theory and Techniques, 1968, 16, (4), pp. 218-227.
5 Zaki, K.A. and Chunming, C.: 'New Results in Dielectric-Loaded Resonators', IEEE Transactions on Microwave Theory and Techniques, 1986, 34, (7), pp. 815-824.
6 Fiedziuszko, S.J., 'Dual-Mode Dielectric Resonator Loaded Cavity Filters', IEEE Transactions on Microwave Theory and Techniques, 1982, 30, (9), pp. 1311-1316.

7 Memarian, M. and Mansour, R.R.: 'Quad-Mode and Dual-Mode Dielectric Resonator Filters', IEEE Transactions on Microwave Theory and Techniques, 2009, 57, (12), pp. 3418-3426.
8 Bakr, M.S., Luhaib, S.W.O., and Hunter, I.C.: 'A Novel Dielectric-Loaded Dual-Mode Cavity for Cellular Base Station Applications', in, 2016 46th European Microwave Conference (EuMC), (2016).
9 Hong, J.S.: 'Couplings of Asynchronously Tuned Coupled Microwave Resonators', IEE Proceedings - Microwaves, Antennas and Propagation, 2000, 147, (5), pp. 354-358.